

## Supplementary Information

# An innovative deep eutectic solvent: Chalcogen bonding as primary driving force

Ruifen Shi<sup>b</sup>, Zeyu Wang<sup>a</sup>, Dongkun Yu<sup>c\*</sup>, Chenyang Wei<sup>a</sup>, Rui Qin<sup>a</sup>, Tiancheng Mu<sup>\*a</sup>

<sup>a</sup>*Department of Chemistry, Renmin University of China, Beijing 100872, China. Email: tcmu@ruc.edu.cn; Tel: +86-10-62514925.*

<sup>b</sup>*Zhejiang Institute of Mechanical and Electrical Engineering Corporation Limited, Hangzhou 310051, China*

<sup>c</sup>*Department of Applied Physics, KTH Royal Institute of Technology, Hannes Alfvéns väg 12, 11419, Stockholm, Sweden.*

## Table of Contents

1. Supplementary	Figures	and
Discussion.....	2	
2. Table.....		16
3. References .....		
19		

## 1. Supplementary Figures and Discussion

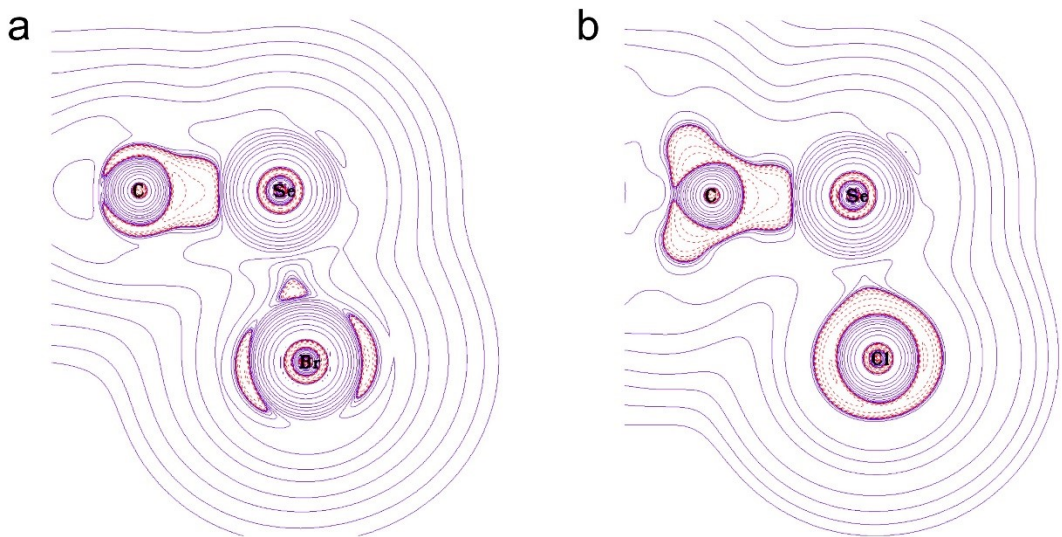
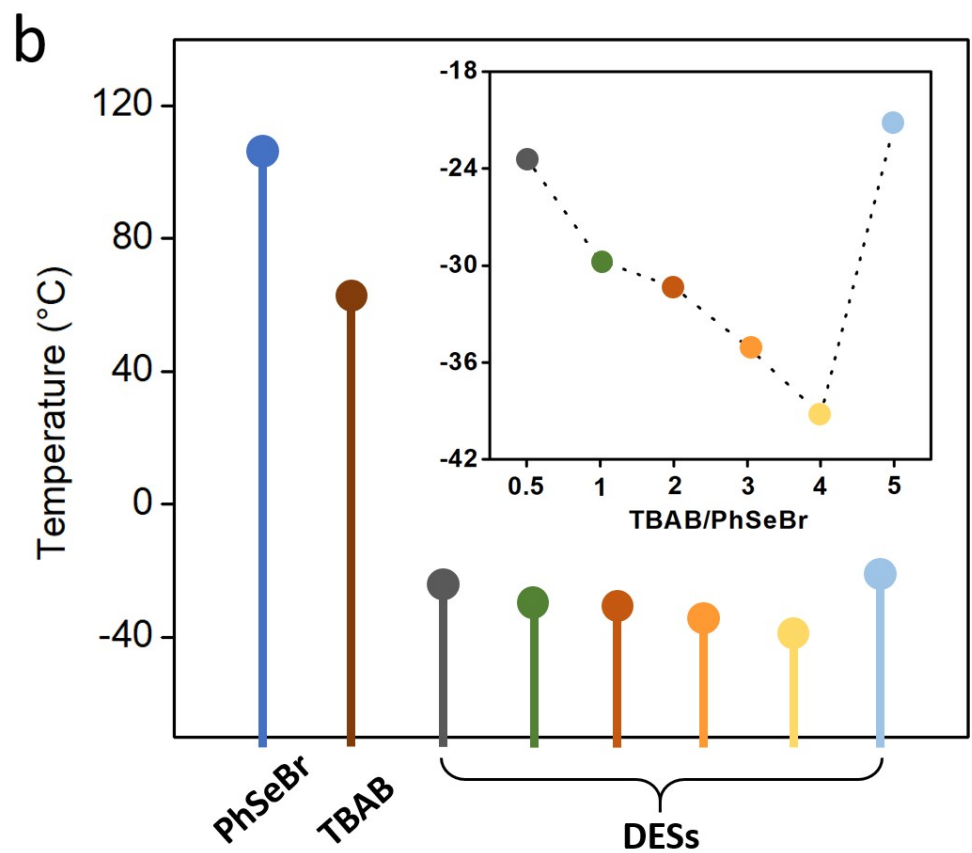
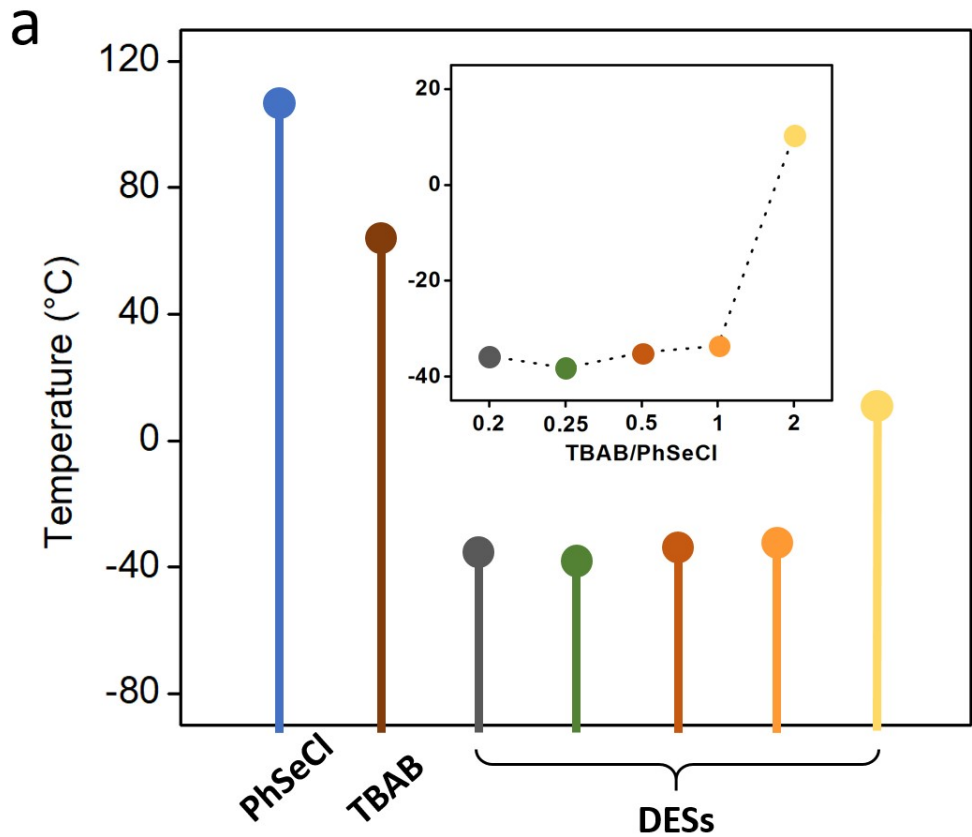


Fig. S1. The 2D contour maps of the Laplacian of the electron density ( $\nabla^2\rho$ ) for ChB donors (a) PhSeBr and (b) PhSeCl molecules. The red dash line and purple solid line correspond to the negative and positive zone, respectively. Computational level: M06-2X/def2-SVP.

The topology of the Laplacian of the electron density have been regarded as an effective tool to clarify the noncovalent interaction<sup>1-5</sup>. As shown in Fig. S1a, there are two significant local concentration of electron density in the valence shell charge concentration of Br. For the PhSeCl molecule, the electrons are concentrated around the whole Cl atom. Compared with Br and Cl, around Se atoms belong to a depleted electron density surrounding, which can bind the rich-electronic groups to form the ChB complex.



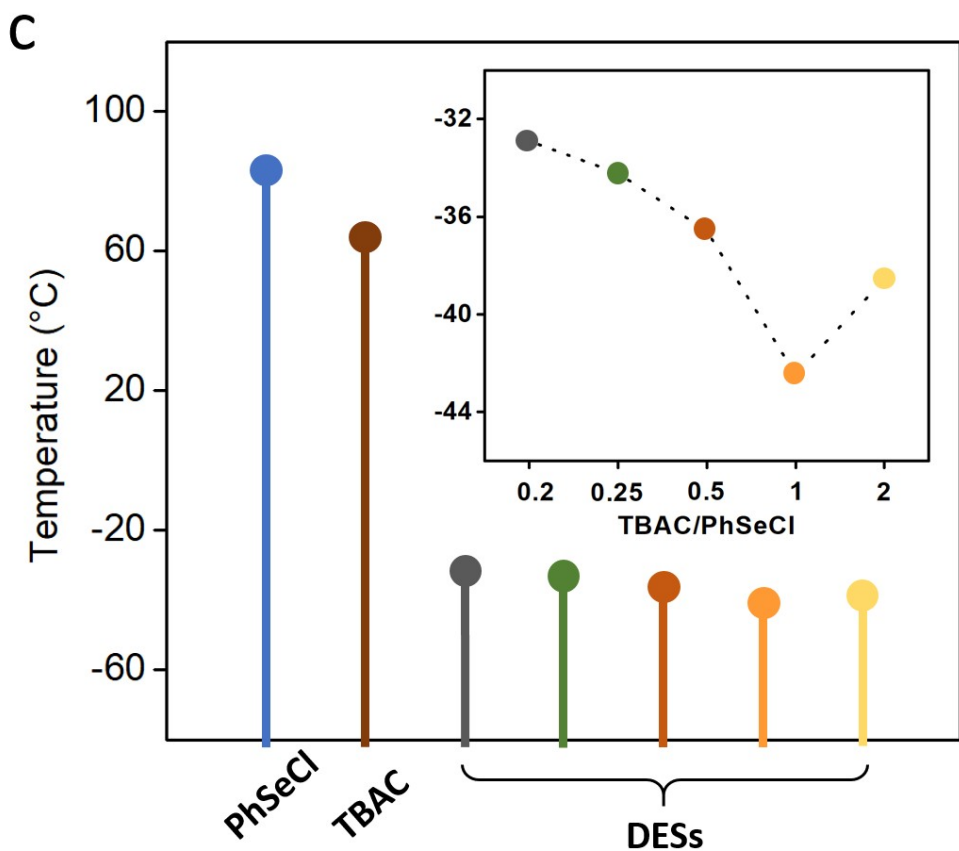


Fig. S2. (a-c) Melting points of other three eutectic systems.

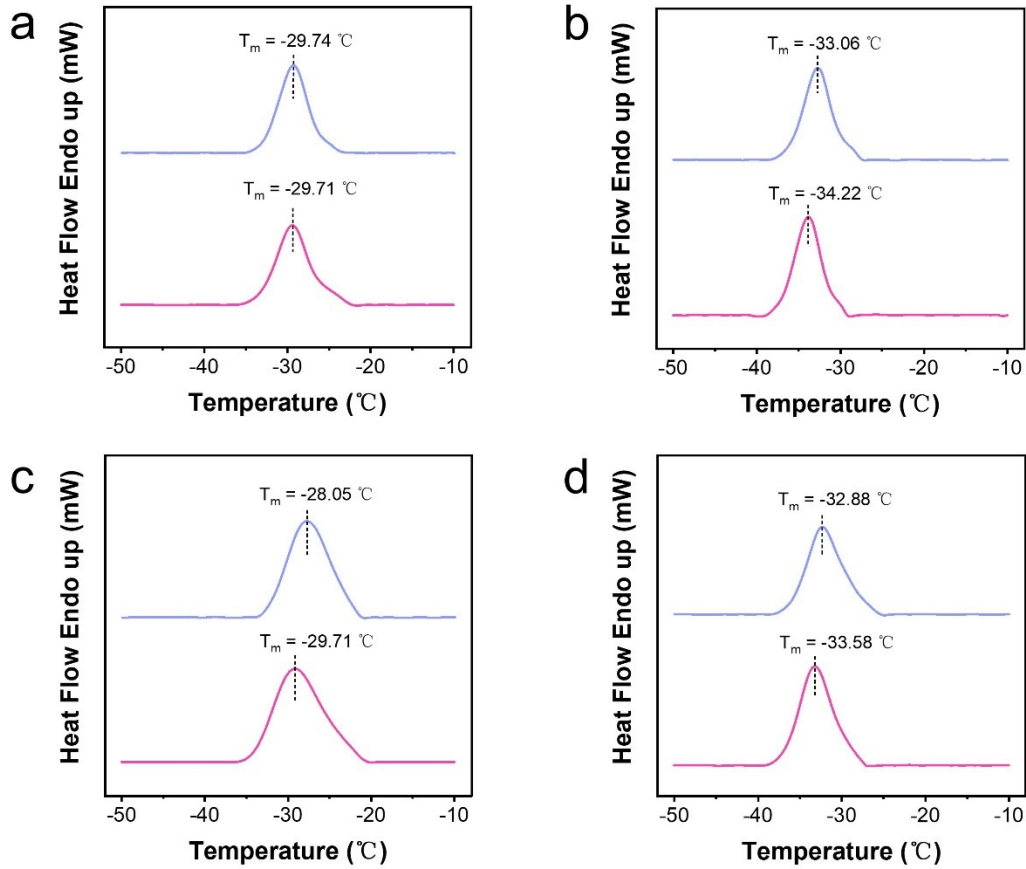


Fig. S3. The thermal behavior of (a)  $(\text{TBAC})_{0.5}(\text{PhSeBr})_{0.5}$ , (b)  $(\text{TBAC})_{0.5}(\text{PhSeCl})_{0.5}$ , (c)  $(\text{TBAB})_{0.5}(\text{PhSeBr})_{0.5}$ , (d)  $(\text{TBAB})_{0.5}(\text{PhSeCl})_{0.5}$  in respective successive cycles. Red and blue lines represent the first and second heating cycles, respectively.

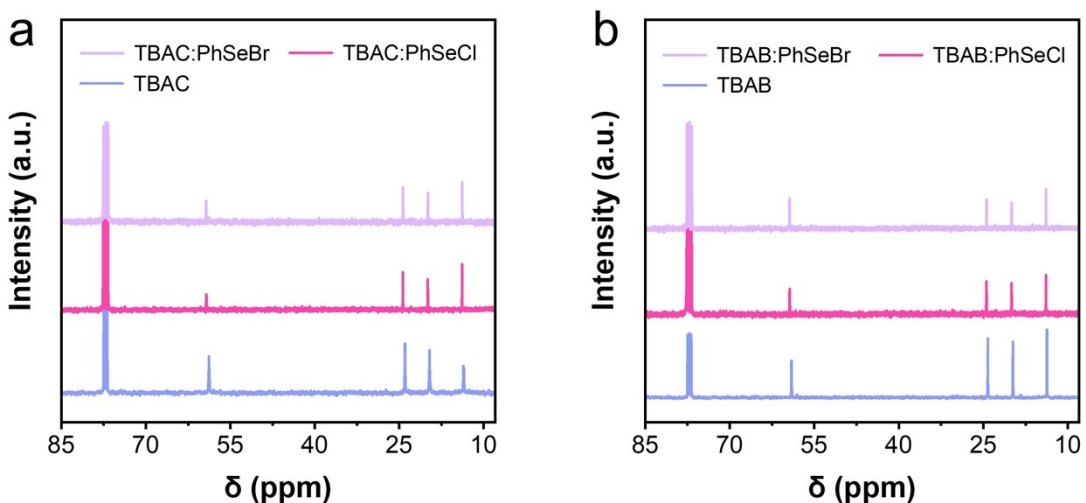


Fig. S4. (a-b) The  $^{13}\text{C}$  NMR spectra of pure TBAC, TBAB, and corresponding ChDES systems (molar ratio 1:1). The solvent is  $\text{CDCl}_3$ .

**TBAC:**  $^{13}\text{C}$  NMR (101 MHz,  $\text{CDCl}_3$ )  $\delta$  77.58, 77.16, 76.74, 58.79, 23.99, 19.63, 13.62

**TBAC+PhSeBr:**  $^{13}\text{C}$  NMR (101 MHz,  $\text{CDCl}_3$ )  $\delta$  77.58, 77.16, 76.74, 59.34, 24.38, 19.96, 13.87

**TBAC+PhSeCl:**  $^{13}\text{C}$  NMR (101 MHz,  $\text{CDCl}_3$ )  $\delta$  77.58, 77.16, 76.74, 59.25, 24.36, 19.95, 13.85

**TBAB:**  $^{13}\text{C}$  NMR (101 MHz,  $\text{CDCl}_3$ )  $\delta$  77.58, 77.16, 76.74, 59.04, 24.20, 19.76, 13.70

**TBAB+PhSeBr:**  $^{13}\text{C}$  NMR (101 MHz,  $\text{CDCl}_3$ )  $\delta$  77.58, 77.16, 76.74, 59.39, 24.43, 19.98, 13.88

**TBAB+PhSeCl:**  $^{13}\text{C}$  NMR (101 MHz,  $\text{CDCl}_3$ )  $\delta$  77.58, 77.16, 76.74, 59.33, 24.40, 19.95, 13.85

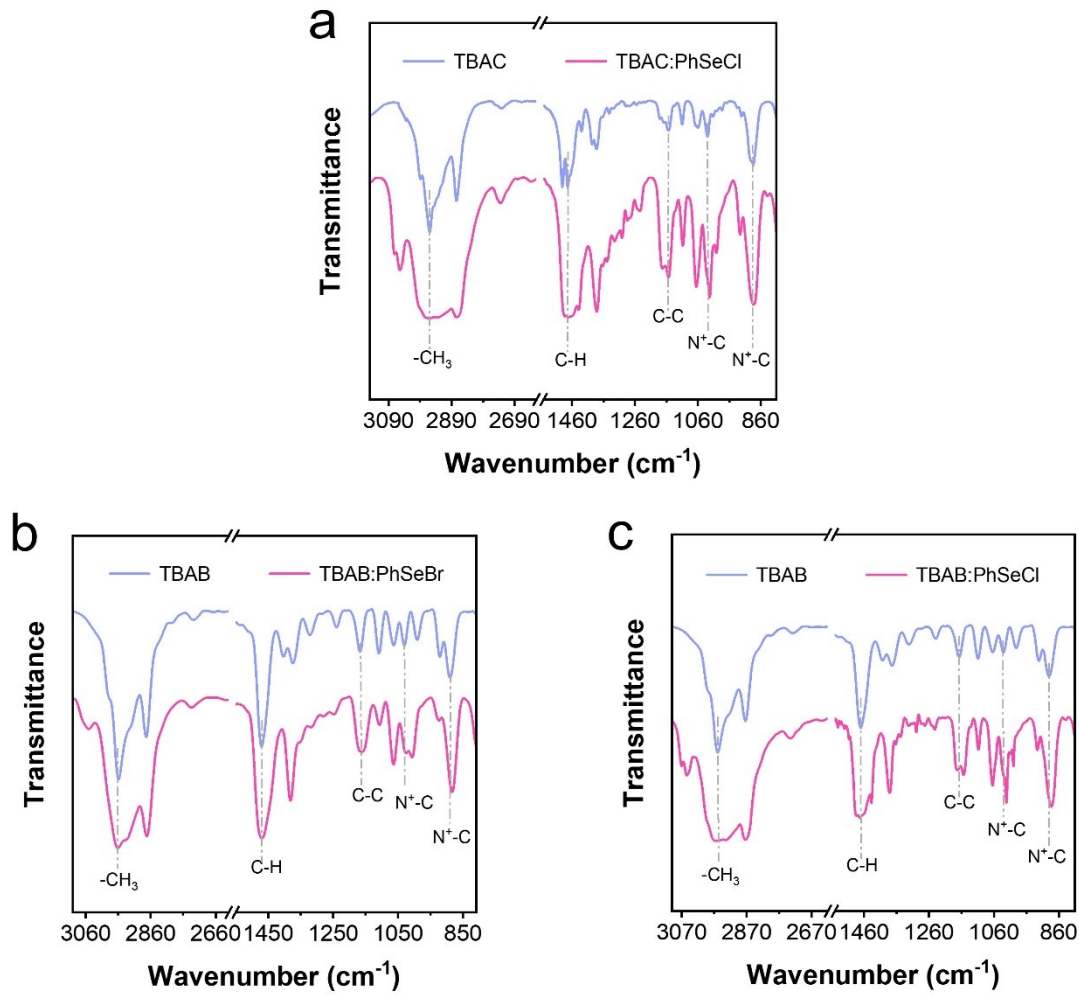


Fig. S5. (a-c) The FTIR spectra of other three ChDESSs (molar ratio 1:1) and corresponding pure components.

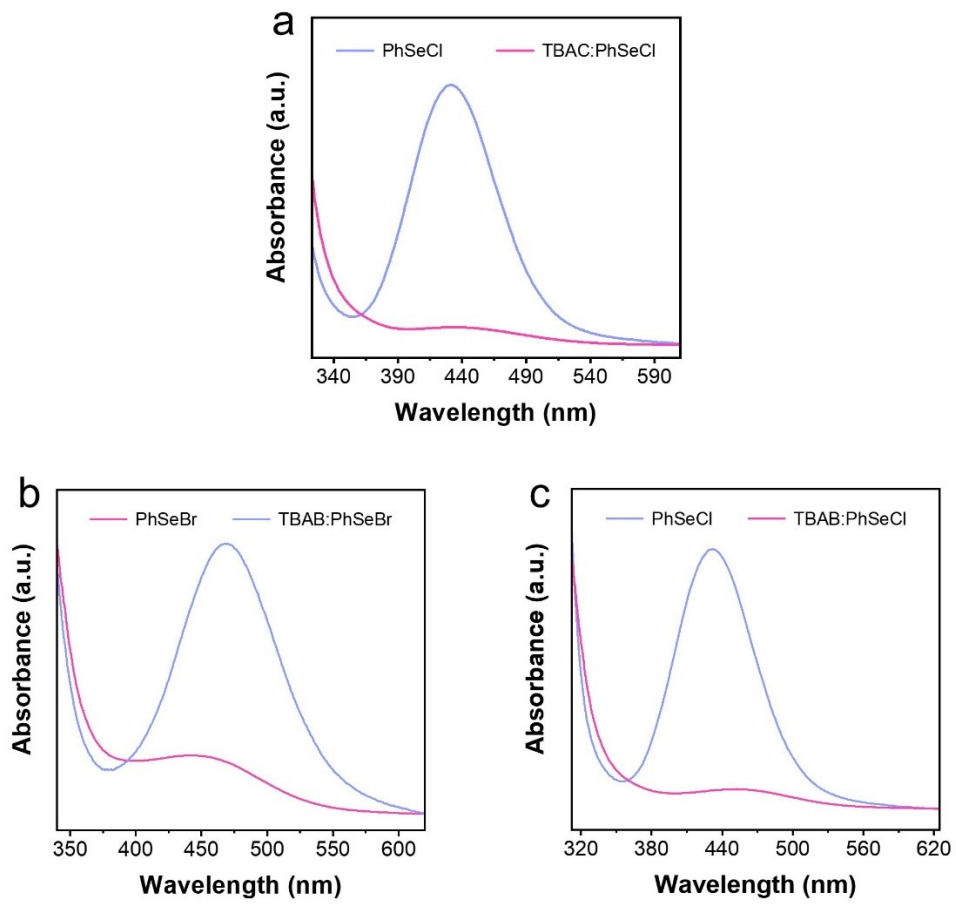


Fig. S6. (a-c) The UV-vis spectra of other three ChDESSs (molar ratio 1:1) and corresponding pure components. The solvent is  $\text{CH}_2\text{Cl}_2$ .

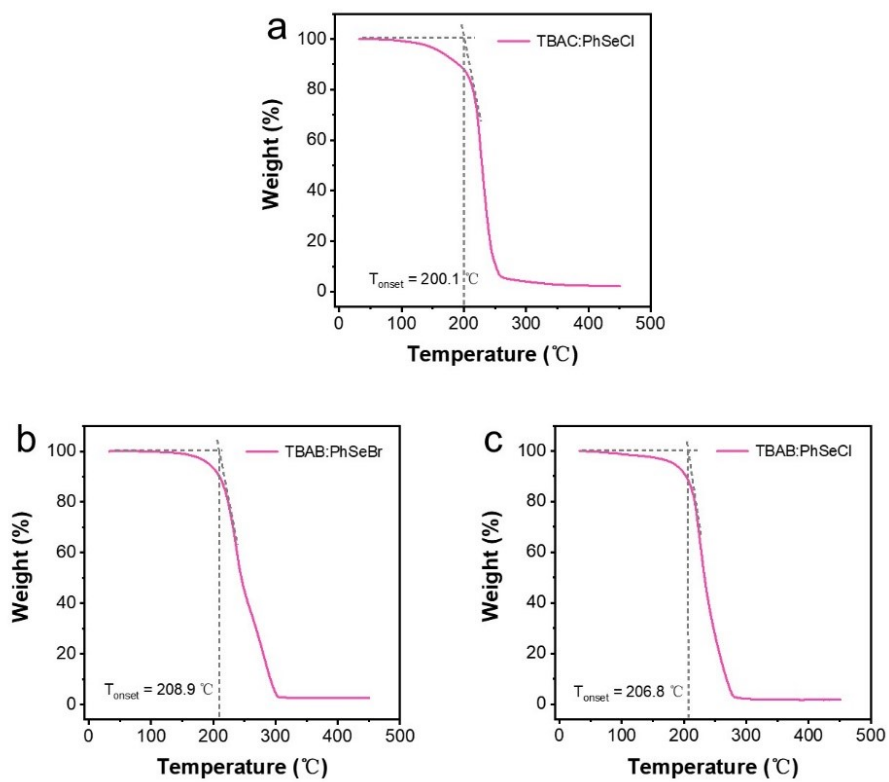


Fig. S7. (a-c) TGA curves of other three ChDESSs (molar ratio 1:1).

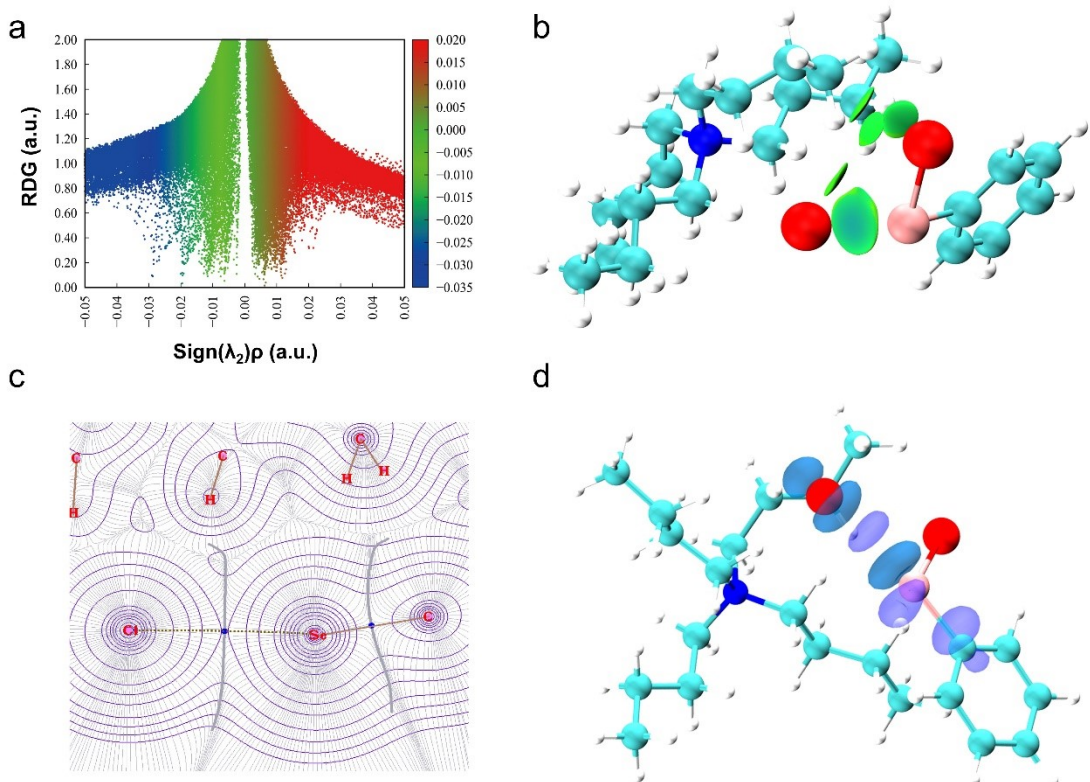


Fig. S8. (a-b) The  $\text{sign}(\lambda_2)\rho$  vs RDG plots and corresponding NCI isosurfaces of  $(\text{TBAC})_{0.5}(\text{PhSeCl})_{0.5}$ . (c) Gradient vector field of the electron density for Se...Cl<sup>-</sup> interaction in  $(\text{TBAC})_{0.5}(\text{PhSeCl})_{0.5}$ . (d) The plot of electron deformation density of  $(\text{TBAC})_{0.5}(\text{PhSeCl})_{0.5}$ .

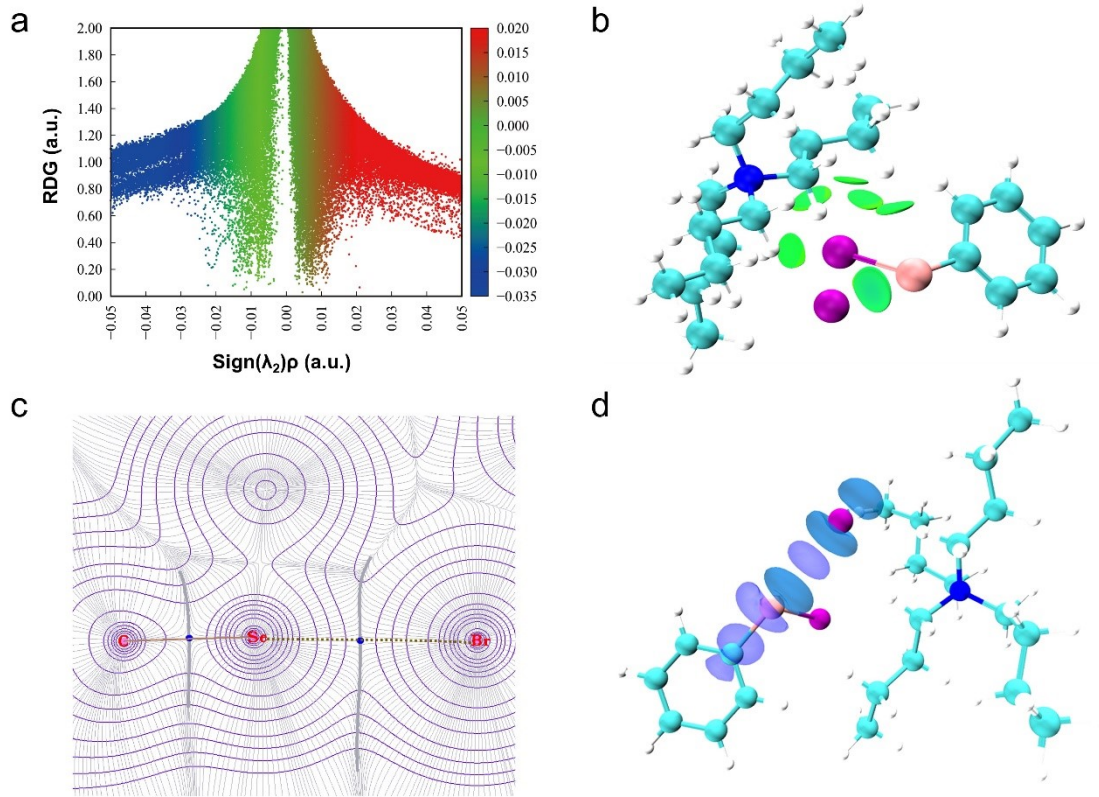


Fig. S9. (a-b) The  $\text{sign}(\lambda_2)\rho$  vs RDG plots and corresponding NCI isosurfaces of  $(\text{TBAB})_{0.5}(\text{PhSeBr})_{0.5}$ . (c) Gradient vector field of the electron density for Se...Br interaction in  $(\text{TBAB})_{0.5}(\text{PhSeBr})_{0.5}$  (d) The plot of electron deformation density of  $(\text{TBAB})_{0.5}(\text{PhSeBr})_{0.5}$ .

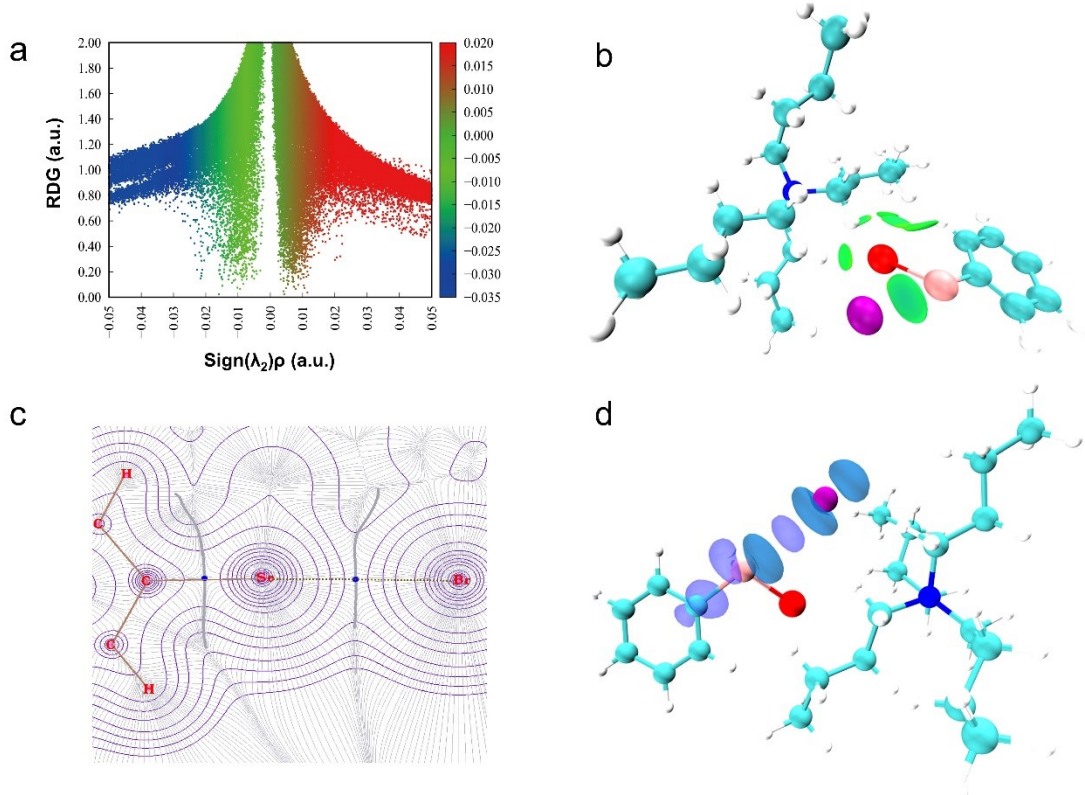


Fig. S10. (a-b) The  $\text{Sign}(\lambda_2)\rho$  vs RDG plots and corresponding NCI isosurfaces of  $(\text{TBAB})_{0.5}(\text{PhSeCl})_{0.5}$ . (c) Gradient vector field of the electron density for Se...Br interaction in  $(\text{TBAB})_{0.5}(\text{PhSeCl})_{0.5}$  (d) The plot of electron deformation density of  $(\text{TBAB})_{0.5}(\text{PhSeCl})_{0.5}$ .

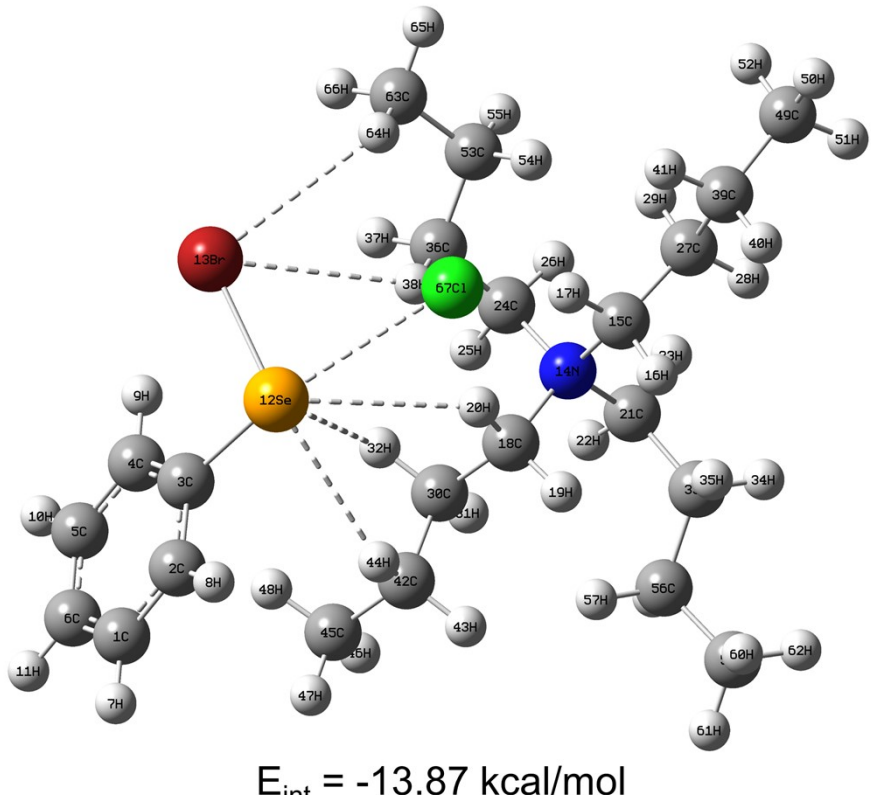


Fig. S11. A diagram of optimized geometries of  $(\text{TBAC})_{0.5}(\text{PhSeBr})_{0.5}$  complex. The chalcogen bond and hydrogen bonds were marked with dash lines and the interaction energy was provided.

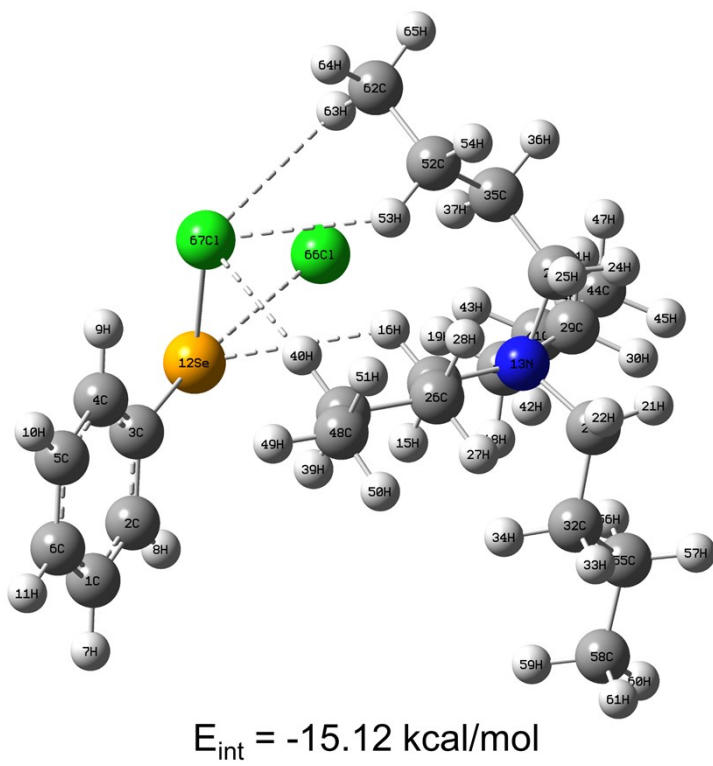
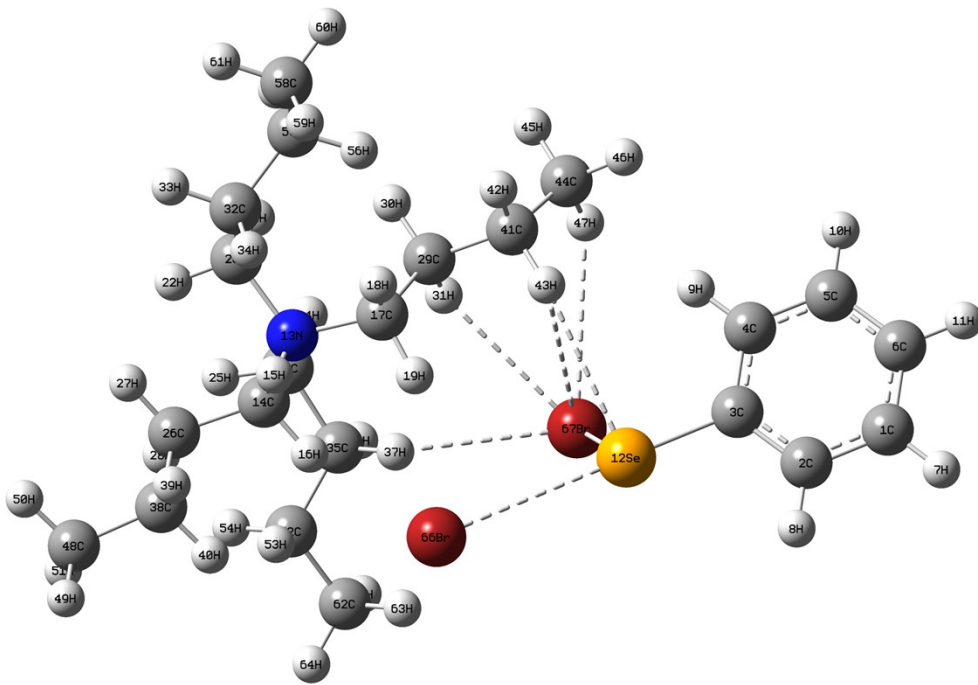
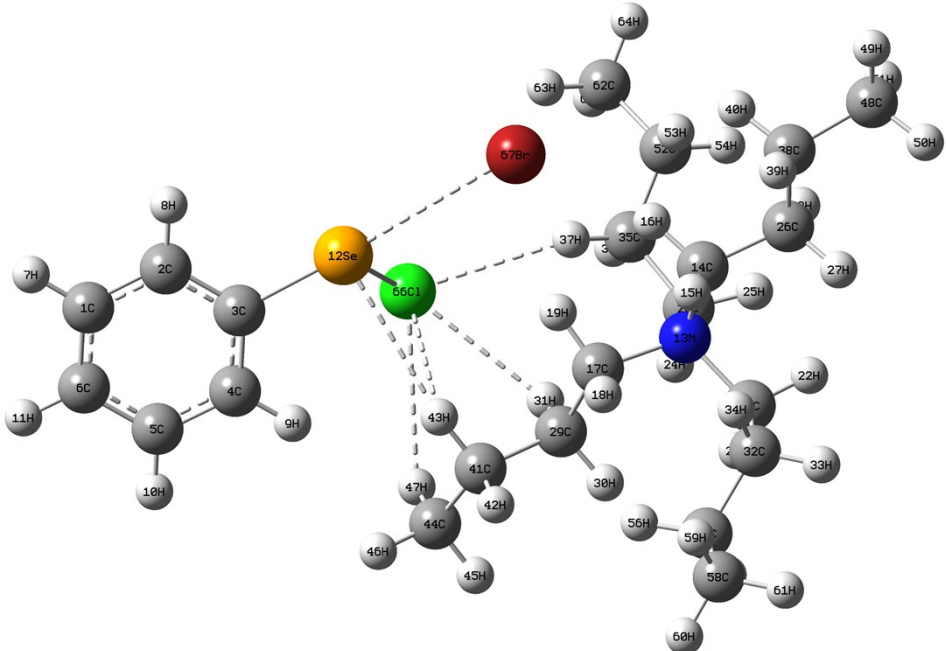


Fig. S12. A diagram of optimized geometries of  $(\text{TBAC})_{0.5}(\text{PhSeCl})_{0.5}$  complex. The chalcogen bond and hydrogen bonds were marked with dash lines and the interaction energy was provided.



$$E_{\text{int}} = -14.31 \text{ kcal/mol}$$

Fig. S13. A diagram of optimized geometries of  $(\text{TBAB})_{0.5}(\text{PhSeBr})_{0.5}$  complex. The chalcogen bond and hydrogen bonds were marked with dash lines and the interaction energy was provided.



$$E_{\text{int}} = -15.62 \text{ kcal/mol}$$

Fig. S14. A diagram of optimized geometries of  $(\text{TBAB})_{0.5}(\text{PhSeCl})_{0.5}$  complex. The chalcogen bond and hydrogen bonds were marked with dash lines and the interaction energy was provided.

## 2. Table

Table S1. IR spectral peaks of pure ChB acceptors and prepared ChDESs (molar ratio 1:1). The value given is corresponding to the peak absorbance of pure components.

Substrate/System	$\nu_{(N^+-C)}$ , $\text{cm}^{-1}$
TBAC	1030, 891
TBAC+PhSeBr	1006, 883
TBAC+PhSeCl	1021, 881
TBAB	1031, 889
TBAB+PhSeBr	1008, 882
TBAB+PhSeCl	1022, 882

Table S2. Some topological properties in a.u at the bond critical point (bcp) of the ChB and HB interactions in the  $(\text{TBAC})_{0.5}(\text{PhSeBr})_{0.5}$  ChDES obtained using the atoms in molecules (AIM) theory by the M06-2X/def2-SVP method. The numberings of the atoms in Table S2 are the same as the Fig. S11.

type	$\rho_{\text{bcp}}^{\text{a}}$ ( $10^{-2}$ )	$\nabla^2 \rho_{\text{bcp}}^{\text{b}}$ ( $10^{-2}$ )	$H_{\text{bcp}}^{\text{c}}$ ( $10^{-3}$ )	$V_{\text{bcp}}^{\text{d}}$ ( $10^{-2}$ )	$G_{\text{bcp}}^{\text{e}}$ ( $10^{-2}$ )	-G/V	E <sup>f</sup>	L <sup>g</sup>	R <sup>h</sup>	$\theta^{\text{i}}$
C3-Se12···Cl <sup>-</sup> 67	1.8	4.6	0.30	-1.1	1.1	1.0	-3.27	3.15	0.85	168.2
C30-H32···Se12	0.69	1.9	0.73	-0.34	0.41	1.2	-0.80	3.20	1.03	111.0
C42-H44···Se12	0.85	2.4	0.75	-0.46	0.54	1.2	-1.15	2.91	0.94	130.6
C18-H20···Se12	0.72	2.1	0.68	-0.39	0.46	1.2	-0.86	3.06	0.99	129.5
C36-H38···Br13	0.63	2.1	0.78	-0.36	0.44	1.2	-0.66	3.11	1.02	118.3
C63-H64···Br13	0.70	2.2	0.86	-0.38	0.46	1.2	-0.82	3.06	1.00	114.8

<sup>a</sup> The electron density. <sup>b</sup> The Laplacian of electron density. <sup>c</sup> The energy density.

<sup>d</sup> The potential electron density. <sup>e</sup> The kinetic energy density.

<sup>f</sup> The bond energy, kcal/mol. <sup>g</sup> The bond length, Å.

<sup>h</sup> 
$$R = \frac{L_{(Se \cdots Cl^-)}}{(r_{Se} + r_{Cl^-})}$$
 where  $r_{Se}$  and  $r_{Cl^-}$  are van der Waals radii of selenium and Pauling ionic radii of chlorine, respectively.

<sup>i</sup> The bond angle, deg.

Table S3. Some topological properties in a.u at the bond critical point (bcp) of the ChB and HB interactions in the  $(\text{TBAC})_{0.5}(\text{PhSeCl})_{0.5}$  ChDES. The numberings of the atoms in Table S3 are the same as the Fig. S12.

type	$\rho_{\text{bcp}}^{\text{a}}$ (10 <sup>-2</sup> )	$\nabla^2 \rho_{\text{bcp}}^{\text{b}}$ (10 <sup>-2</sup> )	$H_{\text{bcp}}^{\text{c}}$ (10 <sup>-3</sup> )	$V_{\text{bcp}}^{\text{d}}$ (10 <sup>-2</sup> )	$G_{\text{bcp}}^{\text{e}}$ (10 <sup>-2</sup> )	-G/V	E <sup>f</sup>	L <sup>g</sup>	R <sup>h</sup>	$\theta^{\text{i}}$
C3–Se12···Cl <sup>−</sup> 66	2.0	4.9	0.092	-1.2	1.2	1.0	-3.72	3.09	0.83	168.4
C14–H16···Se12	0.75	2.2	0.72	-0.40	0.47	1.2	-0.93	3.04	0.98	121.2
C52–H53···Cl67	0.86	2.6	0.49	-0.56	0.60	1.1	-1.18	2.85	0.97	128.5
C38–H40···Cl67	1.1	3.0	-0.18	-0.66	0.79	1.2	-1.71	2.69	0.91	159.4
C62–H63···Cl67	0.63	2.5	1.2	-0.38	0.50	1.3	-0.66	3.03	1.03	104.2

Table S4. Some topological properties in a.u at the bond critical point (bcp) of the ChB and HB interactions in the  $(\text{TBAB})_{0.5}(\text{PhSeBr})_{0.5}$  ChDES. The numberings of the atoms in Table S4 are the same as the Fig. S13.

type	$\rho_{\text{bcp}}^{\text{a}}$ (10 <sup>-2</sup> )	$\nabla^2 \rho_{\text{bcp}}^{\text{b}}$ (10 <sup>-2</sup> )	$H_{\text{bcp}}^{\text{c}}$ (10 <sup>-3</sup> )	$V_{\text{bcp}}^{\text{d}}$ (10 <sup>-2</sup> )	$G_{\text{bcp}}^{\text{e}}$ (10 <sup>-2</sup> )	-G/V	E <sup>f</sup>	L <sup>g</sup>	R <sup>h</sup>	$\theta^{\text{i}}$
C3–Se12···Br <sup>−</sup> 66	1.5	3.8	0.88	-0.76	0.85	1.1	-2.60	3.33	0.86	177.0
C41–H43···Se12	0.80	2.0	0.32	-0.43	0.47	1.1	-1.04	3.02	0.97	161.8
C29–H31···Br67	0.82	2.3	0.62	-0.46	0.52	1.1	-1.09	2.99	0.98	122.6
C35–H37···Br67	0.82	2.3	0.50	-0.47	0.52	1.1	-1.09	2.95	0.97	135.7
C44–H47···Br67	0.50	1.6	0.66	-0.26	0.32	1.2	-0.37	3.27	1.07	122.4
C41–H43···Br67	0.72	2.4	0.84	-0.43	0.51	1.2	-0.86	3.07	1.01	116.4

Table S5. Some topological properties in a.u at the bond critical point (bcp) of the ChB and HB interactions in the  $(\text{TBAB})_{0.5}(\text{PhSeCl})_{0.5}$  ChDES. The numberings of the atoms in Table S5 are the same as the Fig. S14.

type	$\rho_{\text{bcp}}^{\text{a}}$ ( $10^{-2}$ )	$\nabla^2 \rho_{\text{bcp}}^{\text{b}}$ ( $10^{-2}$ )	$H_{\text{bcp}}^{\text{c}}$ ( $10^{-3}$ )	$V_{\text{bcp}}^{\text{d}}$ ( $10^{-2}$ )	$G_{\text{bcp}}^{\text{e}}$ ( $10^{-2}$ )	-G/V	E <sup>f</sup>	L <sup>g</sup>	R <sup>h</sup>	$\theta^i$
C3–Se12···Br <sup>−</sup> 67	1.6	4.0	0.88	-0.82	0.91	1.1	-2.83	3.29	0.85	177.2
C41-H43···Se12	0.80	2.1	0.42	-0.45	0.49	1.1	-1.04	3.01	0.97	160.0
C29-H31···Cl66	0.95	3.0	0.67	-0.62	0.69	1.1	-1.38	2.77	0.94	119.2
C35-H37···Cl66	0.96	2.8	0.28	-0.60	0.66	1.1	-1.40	2.77	0.94	137.8
C44-H47···Cl66	0.51	1.9	0.94	-0.29	0.39	1.3	-0.40	3.14	1.06	118.7
C41-H43···Cl66	0.90	3.2	0.87	-0.62	0.70	1.1	-1.27	2.84	0.96	115.8

The bond energy (E) is also an important parameter to characterize the non-covalent bond strength. Here, we adopted the current more reliable and universal calculation for predict the HB and ChB binding energy based on electron density at corrsponding BCP<sup>6</sup>:

$$E \approx -223.08 \times \rho(r_{BCP}) + 0.7423$$

### 3. References

1. K. Eskandari and M. Lesani, *Chem. Eur. J.*, 2015, **21**, 4739-4746.
2. K. Eskandari and N. Mahmoodabadi, *J. Phys. Chem. A*, 2013, **117**, 13018-13024.
3. P. Popelier, *Coordination Chemistry Reviews*, 2000, **197**, 169-189.
4. L. Tian and C. Qinxue, *Acta Phys. -Chim. Sin.*, 2018, **34**, 503-513.
5. P. R. Varadwaj, A. Varadwaj, H. M. Marques and P. J. MacDougall, *Phys. Chem. Chem. Phys.*, 2019, **21**, 19969-19986.
6. S. Emamian, T. Lu, H. Kruse and H. Emamian, *Journal of computational chemistry*, 2019, **40**, 2868-2881.